Assessing how electroporation affects the effective conductivity tensor of biological tissues

M. Essone Mezeme,[1] M. Kranjc,[2] F. Bajd,[3] I. Serša,[3] C. Brosseau,[1,a)] and D. Miklavčič[2]
[1]*Université Européenne de Bretagne, Université de Brest, Lab-STICC, CS 93837, 6 avenue Le Gorgeu, 29238 Brest Cedex 3, France*
[2]*University of Ljubljana, Faculty of Electrical Engineering, Trzaska 25, 1000 Ljubljana, Slovenia*
[3]*Institut "Jožef Stefan," Jamova cesta 39, 1000 Ljubljana, Slovenia*

(Received 11 July 2012; accepted 31 October 2012; published online 21 November 2012)

We report calculations of the anisotropy ratio of the electrical conductivity of a simple model of a loose connective biological tissue described as a random assembly of multiscale undeformable core-shell and controlled polydisperse spherical structures. One can estimate a 10% increase in the anisotropy ratio due to the application of electric field (duration 100 μm) above the electroporation threshold (40 kV m^{-1}) up to 120 kV m^{-1}. These findings are consistent with the experimental data on the field-induced anisotropy dependence of the electrical conductivity due to cell membrane electroporation. © *2012 American Institute of Physics*. [http://dx.doi.org/10.1063/1.4767450]

There has been a long-standing difficulty to model the interaction of large electric fields with biological tissues.[1–3] The reason is that treating all degrees of freedom in these multiscale systems with strongly correlated cells is a daunting task. In a previous Letter, we have shown by computational means that despite differences in length scales and density, random ternary core-shell sphere packings with different spatial scales can provide a basis for detailed analysis of the electroporation (EP) of tissues.[4] A particularly interesting feature of this method is that it allows for efficient evaluation of temporal evolution of the electrical conductivity of these packings during application of an electric field with magnitude either below or above the value leading to cell membrane EP. It has been pointed out that it predicts a sigmoidal electric field-dependent fraction of electroporated cells which is consistent with what is observed experimentally.

So far, the bulk of theoretical and experimental efforts along these lines has focused on using scalar permittivity and electrical conductivity. Very little is known at this point about the anisotropy properties of biological tissues. The number of reported experimental studies of permittivity and electrical tensors of biological tissues is not large, e.g., see Refs. 5–7. Much attention has been focused on high-resolution microelectrode arrays that allow electrical characterization of tissues noninvasively with large spatiotemporal resolution.[7] Tuch and co-workers[8] showed how the electrical conductivity tensor of tissue can be quantitatively inferred from the water self-diffusion tensor as measured by diffusion tensor magnetic resonance imaging (MRI). Recent advances in transport measurements, coupled to the development of models, revealed the existence of a small anisotropy in the conductivity above a threshold value of the induced transmembrane voltage (ITV_{th}). In fact, the authors reporting conductivity anisotropy results noted a $\approx$10% difference between two perpendicular electric field orientations.[5,6]

The aim of the simulations described in this letter was to search for estimating the anisotropy ratio of the conductivity tensors of such biological materials. As well as being important in their own right, our analysis also provides a useful testbed for identifying important features of EP, determining what causes it, and finding the range of parameters over which it applies.

We performed a set of numerical experiments based on the asymptotic DeBruin-Krassowska (DBK) model of EP for a single cell based on the Smoluchowski equation.[6,9] Though we lack a general microscopic theory linking transport properties and the hierarchy of the cell's microstructure, this approach not only has the virtue of being very general but is also able to describe the electric shock-induced changes in transmembrane potential, which is of crucial importance for EP. Here and throughout the letter, we will restrict attention to undeformable spherical cells modelled as a core-shell (CS) structure. Schwan[10] laid the groundwork in understanding the properties of such CS models of cells with known size, shape, and distribution of charges. Representative values for the primary parameters defining the assembly of CS structures and the cell and tissue EP are identical to those of Table I in Ref. 11. The geometry we consider is depicted schematically in Fig. 1(a). The self-consistent method we use to characterize transport properties has been extensively described in the literature (see, e.g., Refs. 2–4 and references therein) and details will not be given here, except where crucial. We consider the case where a uniform external electric field pulse (100 μs), with magnitude E and rise time $t_r = 0.1$ μs, is applied along the x-axis. Since the conductivity $\vec{\vec{\sigma}}$ tensor is independent of the precise boundary conditions imposed on the electrical potential, we can choose those conditions such that $\vec{\vec{\sigma}} = \begin{bmatrix} \sigma_{xx} & 0 & 0 \\ 0 & \sigma_{yy} & 0 \\ 0 & 0 & \sigma_{yy} \end{bmatrix}$, in the Cartesian coordinate system defined by the dielectric axis. We have performed finite element simulations of the σ_{xx} and σ_{yy} components of $\vec{\vec{\sigma}}$. To obtain σ_{yy}, a perpendicular electric field pulse (100 μs) in the y direction is superimposed to the field in the x direction. Typical results of these simulations are shown in Figs. 2 and 3. To be specific, the cell is modelled by using a simple CS structure with membrane thickness of 5 nm, membrane conductivity of 5×10^{-7} Ω^{-1}m^{-1},

a)E-mail: brosseau@uiv-brest.fr.

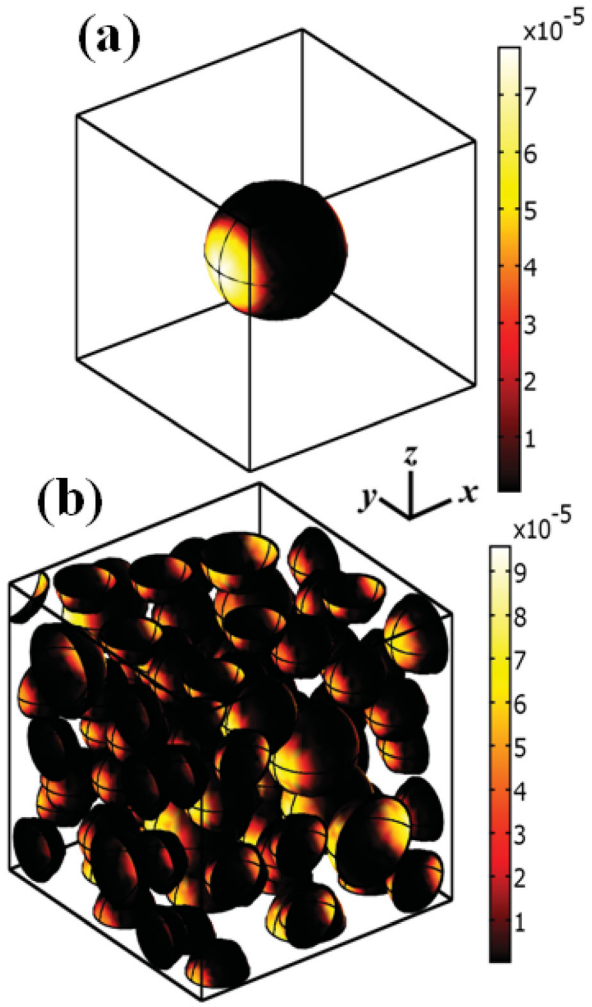

FIG. 1. (a) A single cell in the computational domain. (b) Illustrating the random ternary CS sphere packings studied, with three cell radii 8, 10, and 12 μm, corresponding to a volume fraction of cell inside the computational domain set to 33 vol. %.

intracellular conductivity of 0.2 $\Omega^{-1}m^{-1}$, and extracellular conductivity of 0.127 $\Omega^{-1}m^{-1}$. These numbers are comparable to related theoretical calculations.[2–4,6,9,10] To model simply a tissue as a random assembly of multiscale CS spherical structures, we have considered three cell radii 8, 10, and

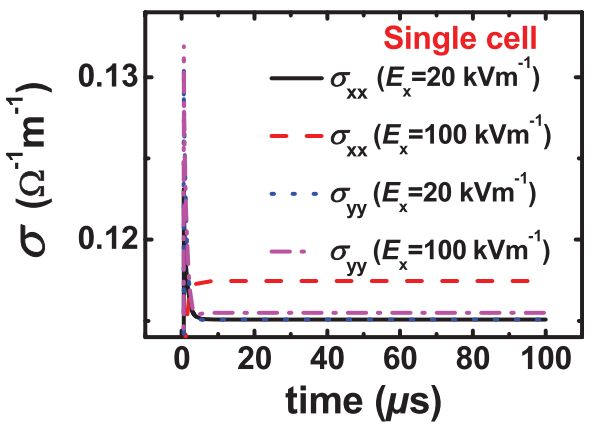

FIG. 2. (a) Simulation results for the electrical conductivity of a single cell as a function of time for the electroporated (solid line) and non-electroporated (dashed line) cell membrane subjected to the applied electric field. (b) Same for the effective conductivity. The field duration is 100 μs.

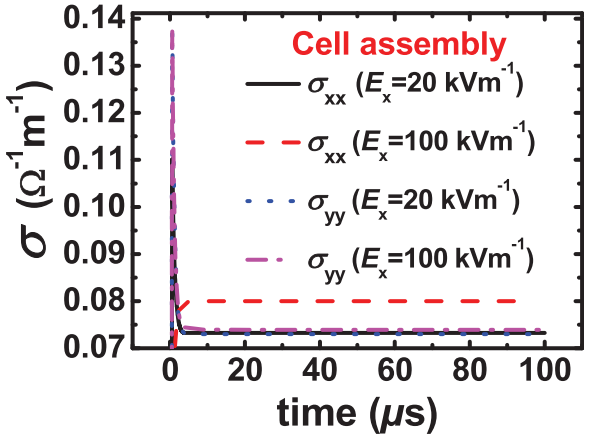

FIG. 3. Same as in Fig. 2 for the average of five realizations of the random ternary CS sphere packing with different spatial scales modelling a tissue. The volume fraction of cell inside the computational domain is set to 33 vol. %. The field duration is 100 μs.

12 μm. These values are consistent with the cell size distribution observed in reflectance in biological tissues.[12] The cubic computational domain (condenser) is filled by a homogeneous medium (whose dielectric properties are assimilated to water) in which nonoverlapping spherical cells are distributed randomly but uniformly. In the actual numerical calculations, the volume fraction of cell is held constant and is set to 33 vol. %. Because of the large computational effort for modelling three dimensional heterostructures, we limit ourselves to study five realizations of the random assembly of cells. The average computational time of a typical simulation of the multicellular tissue model shown in Fig. 1(b) is about 1 h. Most computational parameters are the same as those used in our earlier work.[4] As long as the quasistatic approximation is valid, all of the tensor components are calculable in this continuous effective medium approach. We use finite element as implemented in COMSOL MULTIPHYSICS,[13] using a $80 \times 80 \times 80\ \mu m^3$ computational domain with electrically insulated boundary conditions for the *x-y* and *x-z* planes (conservation of the electric current density). The average cell number is 82 for the 5 realizations of the model and the density is 1.6×10^{14} cells/m^3.

Experimental measurement of the anisotropy ratio of the conductivity tensor using magnetic resonance electrical impedance tomography (MREIT) was also performed. MREIT is based on reconstructing images of true conductivity with high spatial resolution by obtaining current density information using magnetic resonance imaging (MRI) and measuring surface voltage potential.[14–16] Even though reconstructed conductivity images are mostly assessed by multiple injections of low current, it was showed recently that single electroporation pulses are also applicable for reconstruction.[17] We performed *ex vivo* measurement on fresh chicken liver tissue obtained from a slaughterhouse (Perutnina Ptuj, d.d., Ptuj, Slovenia) which operates in accordance to Slovenian law (Ur.l. RS, N. 5/2006). We placed cylindrically shaped tissue samples inside an Oxford 2.35 T horizontal bore superconducting magnet (Oxford instruments, U. K.) and expose it to 1.5 ms long electric pulses with amplitude of 1400 V using an electroporator Jouan GHT 1287 (Jouan, France). *Ex*

vivo tissue samples were exposed to electric field with strength ranging from 20 kV m^{-1} up to 250 kV m^{-1} in areas which were distant to, or near, the electrodes, respectively. MRI of current induced magnetic field changes inside tissue sample was acquired using the two-shot RARE CDI sequence.[17] Afterwards, we reconstructed electrical conductivity using MREIT J-substitution algorithm which is based on solving iteratively Laplace's equation. More details on the methodology can be found in Ref. 17. Measurements were repeated ten times and each sample was replaced with a fresh one after each electroporation pulse delivery to ensure identical initial conditions.

We start by discussing the simpler case of a single cell (Fig. 1(a)). The results are summarized in Fig. 2. In this figure, two curves are shown for the effective conductivity below (20 kVm^{-1}) or above (100 kVm^{-1}) the EP threshold (40 kVm^{-1}). Below the EP threshold, the results yield superimposable conductivity values (solid and dotted lines) plotted as a function of time. When a perpendicular field is applied above the EP threshold, our simulations predict discrimination compared to the conductivity obtained from the parallel case. These results were also obtained in Ref. 6 and are qualitatively similar to those of Huclova and coworkers.[18]

We now consider random ternary CS sphere packings with different spatial scales, as shown in the illustrative case of Fig. 1(b). We are faced with two serious challenges: first, the spatial heterogeneity of the random distribution of cells within the computational domain must be dealt with. Second, an ensemble average is taken over many different realizations that have the same boundary conditions. We are, however, able to circumvent these issues by using the analysis described in Ref. 4. The results are summarized in Fig. 3 for the average conductivity of the random ternary CS sphere packings. In Fig. 3, we present data showing the evolution of the average electrical conductivity as a function of time below or above the EP threshold. The anisotropy that we describe in Fig. 3 is a statistical property of an ensemble of realizations, whereas the behavior shown in Fig. 2 is the manifestation of this anisotropy for a single cell. It is also worth observing that the initial spikes observed in Figs. 2 and 3 correspond to the capacitive term of the current. Their amplitude gets more pronounced with shorter rise time of applied electric pulses.[19]

Fig. 4 further illustrates the effects of raising electric field amplitude on anisotropy ratio of the electrical conductivity defined as $\Delta\sigma = (\sigma_{xx} - \sigma_{yy})/\sigma_{xx}$ for our model of tissue. It can be immediately seen that as electric field increases from 40 to 160 kVm^{-1}, the ratio increases from ≈0% to 14% monotonically with a significant upturn at 60 kVm^{-1}. The question that remains now regards the mechanism promoting the field-induced anisotropy, whether it is driven by the anisotropy intrinsic to the individual cell, or that related to the randomness and connectedness of the tissue. The small anisotropy, ≈3%, observed in Fig. 2 immediately suggests that the electric field dependence of the anisotropy ratio is mainly determined by the collective behavior associated with the cell membrane EP of dense cell suspensions. One additional observation is worthy of note. Fig. 4 shows also the dimensionless parameter

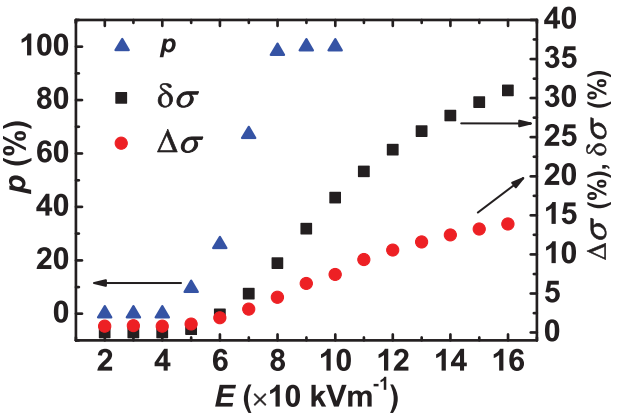

FIG. 4. The anisotropy $\Delta\sigma = (\sigma_{xx} - \sigma_{yy})/\sigma_{xx}$ (full circles) and field $\delta\sigma = (\sigma_E - \sigma_{E_0})/\sigma_{E_0}$ (full squares) ratios of the averaged electrical conductivity tensor components for random ternary CS sphere packing as a function of the applied electric field (left axis). σ_E and σ_{E0} are, respectively, the conductivities calculated with an electric field (in the x-direction) of magnitude set to E and to E_0, respectively. Fraction of electroporated cells p, as a function of electric field magnitude E (right axis, from Ref. 4). The volume fraction of cell inside the computational domain is set to 33 vol. %. $E_0 = 20$ kV m^{-1}. The results are the averages of 5 realizations of the ternary CS tissue model. The field duration is 100 μs.

$\delta\sigma = (\sigma_E - \sigma_{E_0})/\sigma_{E_0}$, which concerns the sole application of an electric field along the x-axis, and where E_0 denotes a reference value for the nonelectroporated state (20 kVm^{-1}), and the fraction of electroporated cells p obtained in Ref. 4 for cell density of 33 vol. %. We observe that even if all cells are electroporated at a field magnitude of 90 kVm^{-1}, $\delta\sigma$ still grows in field, indicating the increase of the electroporated cell's area fraction. It is noted that the anisotropy ratio $\Delta\sigma$ observed for electroporated states is significantly smaller than the field ratio $\delta\sigma$.

Fig. 5 shows the measured anisotropy ratio of the electrical conductivity $\Delta\sigma = (\sigma_{xx} - \sigma_{yy})/\sigma_{xx}$ for liver tissue in the electric field range between 20 kVm^{-1} and 120 kVm^{-1}. It should be noted that the effect of electric field amplitude on $\Delta\sigma$ can be evaluated and compared with simulation results even though the cylindrical geometry of imaging tissue, the electrode type, and the measurement configuration

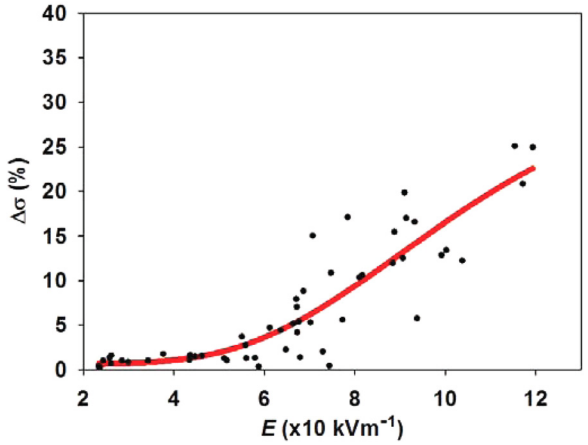

FIG. 5. The anisotropy ratio $\Delta\sigma$ of the averaged electrical conductivity tensor components for a chicken liver tissue. The results (full circles) are the averages of measurements on 10 liver samples. The solid (red) line is a guide to the eyes.

(4 needle electrodes) introduces conditions which differ from the numerical experiment where the electric field was uniformly applied along either the x- or the *y*-axis. Remarkably, the electric field dependence of the measured $\Delta\sigma$ shown in Fig. 5 reproduces the simulated one in Fig. 4. Observe that $\Delta\sigma$ remains practically constant below $\approx$50 kVm^{-1}. In contrast, at higher electric field amplitudes, the data show strong scatter. The observed value of $\approx$50 kVm^{-1} is also similar to the reversible electroporation threshold of rabbit liver determined in an earlier study.[18]

Importantly, the presence of anisotropy in the conductivity agrees qualitatively well with conductivity measurements on single cell.[6] Our results are also in qualitative agreement with recent studies of Gilboa *et al*.[5] using microelectrode arrays where they conclude that the tissue conductivity should present a smooth tensor field. More importantly, the analysis method of this work can serve as an opportunity to understand the EP mechanisms of biological tissues.

In summary, the primary motivation in this study was to analyze a particular model of connective biological tissue described as a random assembly of undeformable core-shell and controlled polydisperse spherical structures. We have applied a methodology that circumvents the numerical difficulties of modeling multiscale media by using three cell radii. We note that the anisotropy ratio of the electrical conductivity does not reach substantial amplitude in simulations, except for electric field magnitude which will eventually compromise the viability of the tissue. The conclusions reached here with regards to the EP properties of tissues are consistent with current and previous experimental investigations.[5]

While the question of generality of the current modelling approach for a tissue remains open, the present results will both motivate further studies and also serve as an important anchor in future discussions of EP. One immediate extension of our study would be to consider a wider range of random filling of the computational domain. We certainly acknowledge that there are subtleties due to the randomness of dense sphere packings; for example, the impact of connectedness and clustering of spheres.[20] Nevertheless, the current results suggest that the current model may be a good approximation of biological tissues, and we take this opportunity to remind the reader that extensive discussions of the effective conductivity tensor of random two-component inhomogeneous materials have appeared in the literature.[20,21] In this respect, we expect that the results presented in this letter will stimulate further work on the applicability of this model to open problems in EP of biological tissues, e.g., relating ITV measurements to the electrophysiological state of cells in the tissue.

M.E.M. acknowledges support from the Conseil Régional de Bretagne (grant programme 211-B2-9/ARED) and the Ph.D. mobility funding of the Université Européenne de Bretagne. The Lab-STICC is Unité Mixte de Recherche CNRS 6285. This work was also partly supported by the Slovenian Research Agency.

[1]G. Emili, A. Schiavoni, M. Francavilla, L. Roselli, and R. Sorrentino, IEEE Trans. Microwave Theory Tech. **51**, 178 (2003).
[2]R. Pethig, *Dielectric and Electronic Properties of Biological Materials* (Wiley, New York, 1979); K. R. Foster and H. P. Schwan, Crit. Rev. Biomed. Eng. **17**, 25 (1989).
[3]K. C. Smith, T. R. Gowrishankar, A. T. Esser, D. A. Stewart, and J. C. Weaver, IEEE Trans. Plasma Sci. **34**, 1480 (2006).
[4]M. Essone Mezeme, G. Pucihar, M. Pavlin, C. Brosseau, and D. Miklavčič, Appl. Phys. Lett. **100**, 143701 (2012).
[5]E. Gilboa, P. S. La Rosa, and A. Nehorai, Ann. Biomed. Eng. **40**, 2140 (2012); C. Gabriel, "Dielectric properties of biological materials," in *Bioengineering and Biophysical Aspects of Electromagnetic Fields*, edited by F. S. Barnes and B. Grenebaum (CRC, New York, 2006).
[6]T. Kotnik, F. Bobanović, and D. Miklavčič, Bioelectrochem. Bioenerg. **43**, 285 (1997); M. Pavlin and D. Miklavčič, Biophys. J. **85**, 719 (2003); M. Pavlin, M. Kandušer, M. Reberšek, G. Pucihar, F. X. Hart, R. Magjarević, and D. Miklavčič, Biophys. J. **88**, 4378 (2005); T. Kotnik and D. Miklavčič, Biophys. J. **90**, 480 (2006); M. Pavlin, V. Leben, and D. Miklavčič, Biochim. Biophys. Acta **1770**, 12 (2007).
[7]L. Berdondini, K. Imfeld, A. Maccione, M. Tedesco, S. Neukom, M. Koudelka-Hep, and S. Martinoia, Lab. Chip **9**, 2644 (2009); K. Imfeld, S. Neukom, A. Maccione, Y. Bornat, S. Martinoia, P. Farine, M. Koudelka-Hep, and L. Berdondini, IEEE Trans. Biomed. Eng. **55**, 2064 (2008); J. Wtorek, A. Bujnowski, A. Poliński, L. Józefiak, and B. Truyen, Physiol. Meas. **25**, 1249 (2004); P. Steendijk, G. Mur, E. T. van der Velde, and J. Baan, IEEE Trans. Biomed. Eng. **40**, 1138 (1993), Y. Wang, P. H. Scimpf, D. R. Haynor, and Y. Kim, IEEE Trans. Biomed. Eng. **45**, 877 (1998).
[8]D. S. Tuch, V. J. Wedeen, A. M. Dale, J. S. George, and J. W. Belliveau, Proc. Nat. Acad. Sci. **25**, 11697 (2001); Ann. N.Y. Acad. Sci. **888**, 314 (1999).
[9]K. A. DeBruin and W. Krassowska, Biophys. J. **77**, 1213 (1999); K. A. DeBruin and W. Krassowska, *ibid*., **77**, 1225 (1999).
[10]H. P. Schwan, Adv. Biol. Med. Phys. **5**, 147 (1957).
[11]G. Pucihar, T. Kotnik, B. Valič, and D. Miklavčič Ann. Biomed. Eng. **34**, 642–652 (2006); G. Pucihar, D. Miklavčič, and T. Kotnik, IEEE Trans. Biomed. Eng. **56**, 1491 (2009); T. Kotnik, G. Pucihar, and D. Miklavčič, J. Membrane Biol. **236**, 3 (2010).
[12]M. Puc, T. Kotnik, L. M. Mir, and D. Miklavčič, Bioelectrochemistry **60**, 1 (2003).
[13]COMSOL MULTIPHYSICS version 3.4 Reference Manual (Comsol AB, Stockholm, Sweden, 2003).
[14]N. Zhang, "Electrical impedance tomography based on current density imaging," M.Sc thesis (Department of Electrical Engineering, University of Toronto, 1992).
[15]E. Degirmenci and B. M. Eyuboglu, Phys. Med. Biol. **52**, 7229 (2007).
[16]J. K. Seo and E. J. Woo, SIAM Rev. **53**, 40 (2011).
[17]M. Kranjc, F. Bajd, I. Sersa, and D. Miklavčič, IEEE Trans. Med. Imaging **30**, 1771 (2011); M. Kranjc, F. Bajd, I. Serša, E. J. Woo, and D. Miklavčič, PLOS One **7**, e45737 (2012).
[18]S. Huclova, D. Erni, and J. Fröhlich, J. Phys. D **43**, 365405 (2010).
[19]D. Cukjati, F. A. Batiuskaite, D. Miklavcic, and L. M. Mir, Bioelectrochemistry **70**, 501 (2007); D. Sel, D. Cukjati, D. Batiuskaite, T. Slivnik, L. M. Mir, and D. Miklavčič, IEEE Trans. Biomed. Eng. **52**, 816 (2005).
[20]S. Torquato, *Random Heterogeneous Materials* (Springer, New York, 2001); M. Sahimi, *Heterogeneous Materials I: Linear Transport and Optical Properties* (Springer, New York, 2003).
[21]O. Levy and D. Stroud, Phys. Rev. B **56**, 8035 (1997); A. Mejdoubi and C. Brosseau, J. Appl. Phys. **99**, 063502 (2006); Phys. Rev. E **74**, 031405 (2006); **73**, 031405 (2006); J. Appl. Phys. **100**, 094103 (2006); V. Myroshnychenko and C. Brosseau, Phys. Rev. E **71**, 016701 (2005); J. Appl. Phys. **97**, 044101 (2005); C. Brosseau, J. Phys. D **39**, 1277 (2006); C. Fourn and C. Brosseau, Phys. Rev. E **77**, 016603 (2008); V. Myroshnychenko and C. Brosseau, J. Phys. D **41**, 095401 (2008); J. Appl. Phys. **103**, 084112 (2008).